Frontiers of Information Technology & Electronic Engineering
www.jzus.zju.edu.cn; engineering.cae.cn; www.springerlink.com
ISSN 2095-9184 (print); ISSN 2095-9230 (online)
E-mail: jzus@zju.edu.cn

An improved method for image denoising based on fractional-order integration*

Li XU[1,2], Guo HUANG[†‡3], Qing-li CHEN[3], Hong-yin QIN[3], Tao MEN[3], Yi-fei PU[2]

[1]*College of Electronics and Materials Engineering, Leshan Normal University, Leshan 614000, China*

[2]*College of Computer Science, Sichuan University, Chengdu 610064, China*

[3]*Key Lab of Internet Natural Language Processing of Sichuan Provincial Education Department, Leshan Normal University, Leshan 614000, China*

[†]E-mail: huangguoxuli@163.com

Received Dec. 24, 2019; Revision accepted Mar. 14, 2020; Crosschecked Aug. 28, 2020

Abstract: Given that the existing image denoising methods damage the texture details of an image, a new method based on fractional integration is proposed. First, the fractional-order integral formula is deduced by generalizing the Cauchy integral, and then the approximate value of the fractional-order integral operator is estimated by a numerical method. Finally, a fractional-order integral mask operator of any order is constructed in eight pixel directions of the image. Simulation results show that the proposed image denoising method can protect the edge texture information of the image while removing the noise. Moreover, this method can obtain higher image feature values and better image vision after denoising than the existing denoising methods, because a texture protection mechanism is adopted during the iterative processing.

Key words: Fractional-order integral; Cauchy integral; Image denoising; Fractional gradient; Texture protection
https://doi.org/10.1631/FITEE.1900727 **CLC number:** TP391

1 Introduction

With the rapid development of computer technology, digital image filtering technology has been widely used. Image denoising is an important part of image filtering. Fractional calculus is an important branch of mathematical analysis (Pu et al., 2014; Shao et al., 2014; Nandal et al., 2018). However, its application in signal analysis and processing, especially in digital image processing, is still a new research direction (Jiang and Wang, 2012; Jalab and Ibrahim, 2015; Yu et al., 2017; Jain et al., 2018). So far, researchers have proposed many conventional methods for image denoising (Chen DL et al., 2013; Zhang GM et al., 2016; Wu GC et al., 2019a). The fractional integral operator weakens the high-frequency part of the signal while preserving the highest-frequency part. Furthermore, it strengthens the low-frequency part of the signal while preserving the lowest-frequency part (Tian et al., 2015; Pu et al., 2016, 2018). Therefore, it can remove noise and retain the edge and texture information of the image so that the denoised image will not produce serious blur (Pu et al., 2008; He et al., 2014; Jalab et al., 2017). The fractional integral operator can effectively suppress the background targets and improve the signal-to-noise ratio (SNR), so that the weak and small targets can be detected (Liu ZJ and Liu, 2007; Zhang J et al., 2012). Liu ST et al.

‡ Corresponding author

* Project supported by the National Natural Science Foundation of China (No. 61201438), the Key Project of Education Department of Sichuan Province, China (No. 18ZA0235), the Research Fund of Key Laboratory of Internet Natural Language Processing of Sichuan Education Department, China (No. INLP201904), and the Research Fund of Leshan Normal University, China (No. LZD003)

ORCID: Li XU, https://orcid.org/0000-0002-1376-1779; Guo HUANG, https://orcid.org/0000-0001-8109-7833

(2001) used the frequency characteristics of the fractional-order integral operator to detect infrared small targets. To solve the problem of losing edge and texture information in the existing image denoising methods, Li and Xie (2016) proposed a new one using a global adaptive fractional-order integral. Liu Y et al. (2011) proposed an integral operator based on the fractional Riemann-Liouville integral, which was applied to digital image denoising, and gave the corresponding algorithm to realize the circuit model of the hardware. Wu XJ et al. (2015) proposed a novel color image encryption algorithm using a fractional-order chaotic system, and compared it with other image encryption schemes. The new algorithm has higher security and is fast for practical image encryption. The discretization representation of the image processing model based on fractional calculus is the key to determine the image processing effect (Chen E et al., 2017; Bai et al., 2018; Wu GC et al., 2019b). Several discretization methods of fractional calculus have been studied in detail and applied to image processing, and good numerical simulation results have been obtained (Amoako-Yirenkyi et al., 2016; Bhrawy and Zaky, 2017; Ding et al., 2017).

To determine the image processing effect, the discretization representation of the image processing model based on fractional calculus should be given. However, the denoising effect is found not to be ideal for images with strong noise, and the integral mask operator has sharp low-pass characteristics because of the relatively large integral order, which will easily destroy the details such as edge and texture of noisy images in the denoising process. The denoising algorithm determines a denoising mask operator constructed by the order of minor integral, and uses multiple iterations to control the effect of image denoising. However, the fractional-order integral operator has low-pass characteristics, and some details of the image will be damaged because of the multi-iteration process.

Denoising effect of traditional denoising methods based on fractional-order integral is not ideal. In this study, an improved fractional-order integral denoising operator is proposed. The basic principle of the image denoising model based on fractional integration is to introduce two parameters, i.e., integral order v and iteration number n. The corresponding image denoising mask can be constructed by setting the micro-integration order, and the local fine-tuning of the noisy image can be realized by combining large iteration numbers. In the iterative denoising process, the fractional gradient modulus of the image is obtained by the fractional differential mask operator of eight pixel directions; then, the intensity of image edge compensation is determined by the classical mathematical model using the fractional gradient modulus as the parameter. Based on this, the denoising algorithm sets a higher order of small integral to construct the denoising mask in the rising stage of the image feature value. Furthermore, it sets a relatively low order of minor integral to construct the denoising mask at the beginning of the decline of the image feature value. The denoising algorithm partially restores the edge and texture information of the image combined with the edge compensation mechanism, maximizes the edge preservation and denoising of the image, and obtains better visual effect.

2 Related work and theory

2.1 Definition of fractional calculus

Fractional calculus is the operation order in the calculus operation which is extended from integer to non-integer. As the basis of fractal geometry and fractal dynamics, it has been widely applied in many areas and achieved remarkable success. Different definitions of fractional calculus can be obtained by analyzing problems from different application perspectives. So far, there is no unified time-domain definition for fractional calculus. Among many definitions, the three classical definitions of fractional calculus are the Grünwald-Letnikov (G-L) definition, the Riemann-Liouville definition, and Caputo definition, as shown in Eqs. (1), (2), and (3), respectively (Podlubny, 1999):

$$ {}_{a}^{\mathrm{G}}I_{t}^{v}=\lim_{h\to 0}h^{v}\sum_{j=0}^{(t-a)/h}\frac{\Gamma(v+j)}{j!\Gamma(v)}g(t-jh),\ v\in\mathbb{R}^{-}, \quad (1) $$

$$ {}_{a}^{\mathrm{R}}D_{t}^{v}f(x)=\begin{cases}\dfrac{\mathrm{d}^{n}g(x)}{\mathrm{d}x^{n}}, & v=n\in\mathbb{N},\\ \dfrac{\mathrm{d}^{n}}{\mathrm{d}x^{n}}\dfrac{1}{\Gamma(n-v)}\displaystyle\int_{a}^{t}\frac{g(y)}{(x-y)^{v-n+1}}\mathrm{d}y, & 0\le n-1<v<n,\end{cases} \quad (2) $$

$$ {}_a^{\mathrm{C}}D_t^v f(x)=\begin{cases}\dfrac{\mathrm{d}^n g(x)}{\mathrm{d}x^n}, & v=n\in\mathbb{N},\\ \dfrac{\mathrm{d}^n}{\mathrm{d}x^n}\dfrac{1}{\Gamma(v-n)}\displaystyle\int_a^t\frac{g^n(y)}{(x-y)^{n-v+1}}\mathrm{d}y, & \\ 0\le n-1<v<n. & \end{cases} \tag{3}$$

2.2 Fractional gradient formula

Assume that the function $g(x, y)\in\mathbb{R}^{M\times N}$ can be discretized as $g=(g_{i,j})_{i,j=1}^{M\times N}$ according to the distance h=1 in the $M\times N$ plane. Thus, the fractional gradient and fractional gradient modulus of $g(x, y)$ can be obtained as follows:

$$\nabla^v g=\left(\nabla^v g_{i,j}\right)_{i,j=1}^{N}=\left(D_x^v g_{i,j}, D_y^v g_{i,j}\right)_{i,j=1}^{N}, \tag{4}$$

$$\nabla^v g(x,y)=\left(\frac{\partial^v g}{\partial x^v}, \frac{\partial^v g}{\partial y^v}\right). \tag{5}$$

Because in this study we calculate the fractional gradient modulus of an image, it is necessary to consider the neighbor pixels in eight dimensions of the image. Thus, the modulus of the gradient operator of fractional differential is extended to eight dimensions of the image:

$$\begin{aligned}\left|\nabla^v g\right|=\frac{1}{\sqrt{8}}\Bigg[&\left(\frac{\partial^v g}{\partial x_+^v}\right)^2+\left(\frac{\partial^v g}{\partial x_-^v}\right)^2+\left(\frac{\partial^v g}{\partial y_+^v}\right)^2+\left(\frac{\partial^v g}{\partial y_-^v}\right)^2\\ &+\left(\frac{\partial^v g}{\partial x_{45^\circ}^v}\right)^2+\left(\frac{\partial^v g}{\partial x_{135^\circ}^v}\right)^2+\left(\frac{\partial^v g}{\partial x_{225^\circ}^v}\right)^2+\left(\frac{\partial^v g}{\partial x_{315^\circ}^v}\right)^2\Bigg]^{\frac{1}{2}},\end{aligned} \tag{6}$$

where x_+, x_-, y_+, y_-, x_{45°, x_{135°, x_{225°, and x_{315° represent eight dimensions centered at the current pixel, v the order of the fractional-order differential, and $|\nabla^v g|$ the gradient modulus value in the eight dimensions of image pixels.

3 Fractional-order integral denoising model

3.1 Establishment of the fractional-order integral operator

Function $g(x)$ can be obtained according to the definition of the integral formula:

$${}_aI_x^n g(x)=\int_a^{x_1}\int_a^{x_2}\cdots\int_a^{x_{n-1}} g(x_{n-1})\mathrm{d}x_{n-1}\cdots\mathrm{d}x_2\mathrm{d}x_1. \tag{7}$$

Combining Eq. (1) with the inductive hypothesis, we can obtain

$$I^n g(x)=\frac{1}{\Gamma(n)}\int_a^x (x-y)^{n-1} g(y)\mathrm{d}y. \tag{8}$$

The integral order n of the Cauchy integral formula can be extended to fractional order v; that is, the fractional-order Cauchy integral formula can be obtained:

$$I^v g(x)=\frac{1}{\Gamma(v)}\int_a^x (x-y)^{v-1} g(y)\mathrm{d}y. \tag{9}$$

Based on the basic properties of the Cauchy integral formula, the integral order of the integer order is extended to the order of the fractional-order integral. Eq. (9) can be discretized using the basic properties of the integral function, and Eq. (10) can be obtained:

$${}_aI_x^v g(x)=\frac{1}{\Gamma(v)}\sum_{j=0}^{N-1}\int_{jx/N}^{(j+1)x/N}\frac{g(x-y)}{y^{v+1}}\mathrm{d}y. \tag{10}$$

Using the method of slope approximation, the following numerical formula can be obtained for the fractional Cauchy integral:

$$\begin{aligned}{}_aI_x^v g(x)=&\frac{g_{j+1}-g_j}{1+v}[(j+1)^{1+v}-j^{1+v}]+\frac{x^v N^{-v}}{\Gamma(v)}\\ &\cdot\sum_{j=0}^{N-1}\frac{(j+1)g_j-jg_{j+1}}{v}[(j+1)^v-j^v].\end{aligned} \tag{11}$$

The high-dimensional fractional Fourier transform is detachable, so we assume that the fractional-order integral mask operator of a two-dimensional image $g(x, y)$ in any direction can be separated. Therefore, the duration $[a, t]$ of the image $g(x, y)$ is divided equally according to the unit interval. Therefore, assuming h=1, we have N=[(t−a)/h]=t−a and can obtain the numerical formulas for the fractional Cauchy integral in the x and y directions, as

shown in Eqs. (12) and (13), respectively:

$$
\begin{aligned}
{}_{c}I_{x}^{v}g(x,y)=&\frac{g_{i+1,j}-g_{i,j}}{1+v}[(i+1)^{1+v}-i^{1+v}]\\
&+\frac{x^{v}N^{-v}}{\Gamma(v)}\sum_{i=0}^{N-1}\frac{(i+1)g_{i,j}-ig_{i+1,j}}{v}[(i+1)^{v}-i^{v}],
\end{aligned}
\tag{12}
$$

$$
\begin{aligned}
{}_{c}I_{y}^{v}g(x,y)=&\frac{g_{i,j+1}-g_{i,j}}{1+v}[(j+1)^{1+v}-j^{1+v}]\\
&+\frac{y^{v}N^{-v}}{\Gamma(v)}\sum_{j=0}^{N-1}\frac{(j+1)g_{i,j}-jg_{i,j+1}}{v}[(j+1)^{v}-j^{v}].
\end{aligned}
\tag{13}
$$

Digital images have the characteristic of self-similarity: the closer the pixel to the central target, the higher the similarity. The weight functions of Eqs. (12) and (13) cannot have a general term expression, so the computational complexity and accuracy are considered. To simplify the calculation, by setting $\varphi(x)=1/[x(1+x)\Gamma(x)]$, the first four terms ($N$=4) of Eqs. (12) and (13) are taken as the estimated values. The denoising mask based on the fractional Cauchy integral can be obtained; its coefficients are given by

$$
\begin{aligned}
[w_0,w_1,w_2,w_3]=&\varphi(v)[1,2^{1+v}+2v-2,2^{v}v-2^{2+v}\\
&+3^{1+v}+3v2^{v}+1,53^{v}v-2^{2+v}v+23^{v}-2^{1+v}].
\end{aligned}
\tag{14}
$$

3.2 Construction of the denoising model

Having determined the fractional gradient modulus of the image, we now introduce the exponential function $\theta(x)=\exp[(x/k)^{\alpha}]$ to obtain the weight coefficient $\omega_{i,j}$ (Here, k is the boundary factor and α the velocity factor).

The relationship between the fractional gradient modulus and the weighting coefficient can be expressed as

$$
\theta_{i,j}(x)=\exp\left[\left(\frac{\left|\nabla^{v}g_{i,j}\right|}{k}\right)^{\alpha}\right]. \tag{15}
$$

The weight function $\theta(x)$ is a subtraction function in [0, 1], and its decreasing amplitude is controlled by the velocity factor α. The larger the value of α, the faster the curve will fall. k represents the boundary factor, and the weight function $\theta(x)$ decreases more rapidly in the range of $x\in[0, k]$ than in the range of $x\in[k, 1]$.

When θ=0, $g_{i,j}^{n+1}=g_{i,j}^{n}$ can be obtained from

$$
g_{i,j}^{n+1}=g_{i,j}^{n}+\theta_{i,j}\left(\sum_{i=1}^{8}\omega_{i,j}g_{i,j}^{n}-g_{i,j}^{n}\right),\ 0\le\theta_{i,j}\le1, \tag{16}
$$

which means that the pixel is more likely to be an edge; this means that there is no need to deal with the pixel in the denoising process (that is, the pixel value is kept unchanged). When θ=1, $g_{i,j}^{n+1}=\left|\nabla^{v}g^{n}{}_{i,j}\right|$ can be obtained from Eq. (16), which means that the pixel is less likely to be an edge; therefore, the problem of edge protection does not need to be considered in the denoising process, and the maximum denoising is carried out using the fractional-order integral operator. When $0<\theta<1$, the fractional-order integral operator can be used to denoise the image to varying degrees according to the magnitude of the fractional gradient modulus of any pixel of the image; in other words, the edge of the denoised image can be compensated for to a certain extent.

3.3 Denoising process

The execution process of the new denoising model proposed in this study is expressed algorithmically as follows:

Step 1: basic parameter setup

Parameters of the proposed denoising algorithm are as follows: The order of the fractional-order integral is set to v_1=0.02 when SNR increases, and v_2=0.01 when SNR decreases (According to the experimental results in Huang et al. (2011), when the fractional integration order is 0.01 or 0.02, good denoising effect can be obtained after a certain number of iterations). The order of the differential operator for calculating the fractional gradient modulus of the image is set to v=0.8, the boundary factor k=0.1, and the speed factor α=2. The maximum number of iterations is set to 150.

Step 2: image denoising processing

(1) Assume that the noise image is $g^0(x, y)$, and set the fractional-order integral order v_1=0.02 or 0.01 according to the SNR difference of the image after two adjacent denoising processes (The first denoising process is the increasing stage of SNR, so the integral order is v_1=0.02). The denoising mask operator based on the fractional Cauchy integral formula is used to

convolve the noisy image, and the first denoised image $g^1(x, y)$ is obtained.

(2) Calculate the SNR of the denoised image $g^1(x, y)$ and set $g^0(x, y)=g^1(x, y)$.

Step 3: image edge compensation

(1) The noise image $g^0(x, y)$ is processed using a Gaussian low-pass filter, and $g^0(x, y)=g^0(x, y)G_{\mu,\sigma}$.

(2) The fractional differential mask operator constructed by Eq. (11) is used to calculate the fractional gradient modulus $|\nabla^v g|$, which is then smoothed by a Gaussian low-pass filter.

(3) Eq. (12) is used to obtain the coefficient $\theta_{i,j}$ of each pixel of the denoised image $g^1(x, y)$ according to the value range of parameter $\omega_{i,j}$, and the denoised image is compensated for by Eq. (13). The total number of iterations is set to 150, and the absolute value of the SNR difference of the image after two adjacent denoising processes is smaller than the threshold ε. If the iterative termination condition is satisfied, the iteration stops, and the program outputs the final denoised image using edge compensation; if the condition is not satisfied, back to step 2.

4 Simulations and discussion

4.1 Image denoising evaluation index

The simulation platform is MATLAB R2014a, and the test images are a simple synthetic image and a detailed Barbara image. In the simulations, the mean squared error (MSE), SNR, edge preservation index (EPI), and average gradient (AG) are used to quantitatively analyze the denoising performance of the image denoising operator. The superiority of the proposed denoising algorithm is verified when combined with the residual image and horizontal image.

1. MSE and SNR

Suppose that the original noise image is $g(i, j)$ and that the denoised image is $g'(i, j)$ (i=1, 2, …, M; j=1, 2, …, N). Then, MSE between $g(i, j)$ and $g'(i, j)$ is expressed as

$$\mathrm{MSE}=\frac{1}{MN}\sum_{i=1}^{M}\sum_{j=1}^{N}[g(i,j)-g'(i,j)]^2. \tag{17}$$

Similarly, SNR between the original image $g(i, j)$ and the denoised image $g'(i, j)$ can be obtained as

$$\mathrm{SNR}=\log\frac{\sum_{i=1}^{M}\sum_{j=1}^{N}g^2(i,j)}{\sum_{i=1}^{M}\sum_{j=1}^{N}[g(i,j)-g'(i,j)]^2}. \tag{18}$$

2. EPI

EPI describes the ability of the filter operator to maintain the horizontal or vertical edge of the image: the higher the EPI, the better the ability of the operator to keep the edge. EPI is expressed as

$$\mathrm{EPI}=\frac{\sum_{i=1}^{n_{\mathrm{row}}}\sum_{j=1}^{n_{\mathrm{col}}}\left|\Delta_{\mathrm{horizontal}}g_{\mathrm{after}}(i,j)+\Delta_{\mathrm{vertical}}g_{\mathrm{after}}(i,j)\right|}{\sum_{i=1}^{n_{\mathrm{row}}}\sum_{j=1}^{n_{\mathrm{col}}}\left|\Delta_{\mathrm{horizontal}}g_{\mathrm{before}}(i,j)+\Delta_{\mathrm{vertical}}g_{\mathrm{before}}(i,j)\right|}, \tag{19}$$

where n_{row} and n_{col} are the numbers of rows and columns of digital image, respectively, and $\Delta_{\mathrm{horizontal}}$ and $\Delta_{\mathrm{vertical}}$ are the pixel differences in the horizontal and vertical directions of the image, respectively.

3. AG

AG of an image can describe the contrast of details and the change of texture in the image, and thus to a certain extent, it reflects the clarity of the image. AG is expressed as

$$\mathrm{AG}=\frac{1}{MN}\sum_{i=1}^{n_{\mathrm{row}}}\sum_{j=1}^{n_{\mathrm{col}}}\sqrt{\Delta_{\mathrm{horizontal}}f^2(i,j)+\Delta_{\mathrm{vertical}}f^2(i,j)}. \tag{20}$$

4.2 Simulations and theoretical analysis

Figs. 1b and 1c show the denoising effect of the G-L method and the proposed method, respectively, when applied to the Barbara image with Gaussian white noise. Fig. 1 shows that the proposed method has better visual effect than the fractional G-L method, and retains more image details such as edges and textures. Fig. 2 compares the denoising performances of the proposed method and the G-L method. As can be seen from Fig. 2, in the process of image iterative denoising, both SNRs increase with the increase of the number of iterations. After denoising, SNRs of the image increase to a certain peak and then decrease.

The maximum SNR of the proposed method is 18.78 dB, and the corresponding number of iterations is 49; the maximum SNR obtained by the fractional G-L method is 18.27 dB, and the corresponding number of iterations is 79. Therefore, the proposed method can achieve a higher SNR than the fractional G-L method in a smaller number of iterations.

Fig. 3 shows the denoising effect of different image denoising methods. The proposed method can better preserve the edge and texture details of the image while removing the noise than the existing

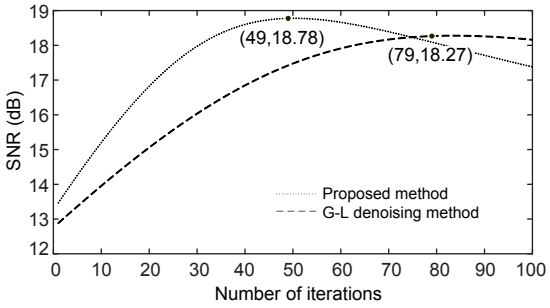

Fig. 2 Denoising performance comparison between the proposed method and the G-L method

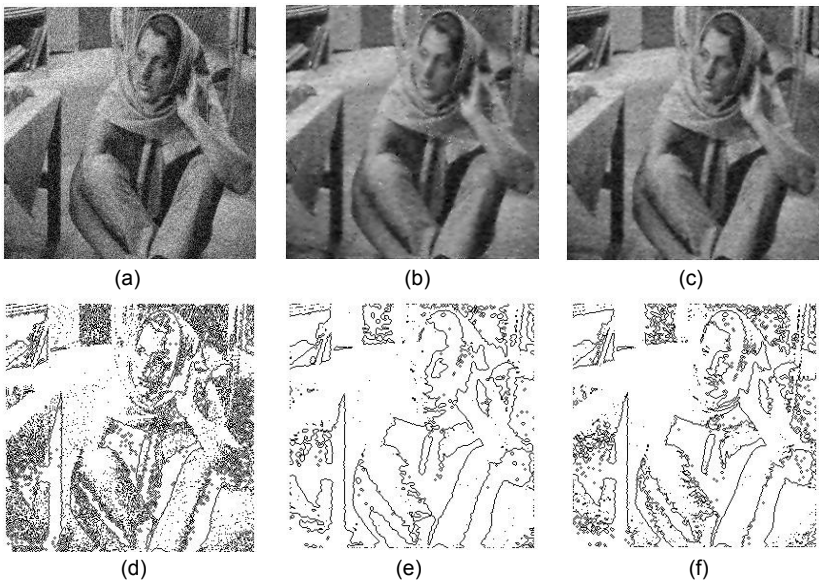

Fig. 1 Noise image (a), denoising effect of the Grünwald-Letnikov (G-L) method (b), denoising effect of the proposed method (c), horizontal line image of the noise image (d), horizontal line image of the G-L method (e), and horizontal line image of the proposed method (f)

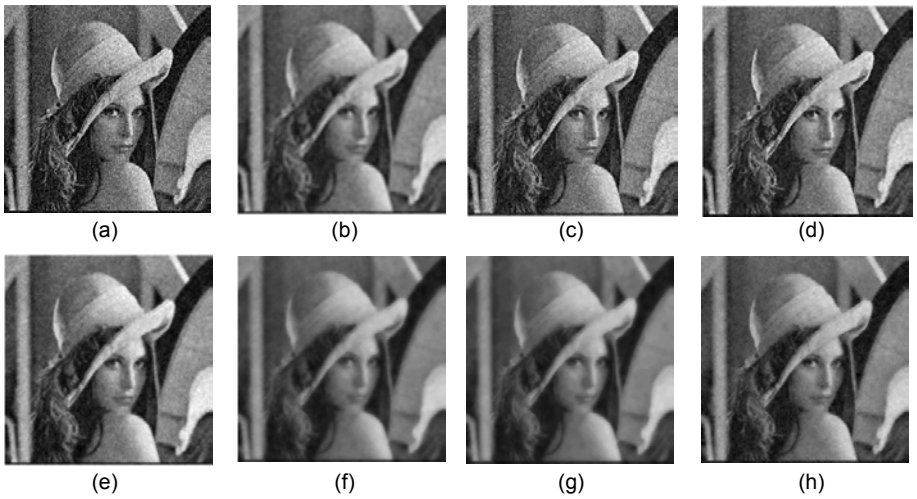

Fig. 3 Noise image (a) and the denoising effect obtained by the mean denoising method (b), Gaussian method (c), Wiener method (d), G-L method (e), PDE method (f), NLM method (g), and the proposed method (h)

classical image denoising methods, and the visual effect of the processed image is better. Fig. 4 shows the horizontal line images of different image denoising methods. The existing denoising methods either cannot effectively remove image noise or seriously blur the edges and contours of the denoised image, whereas the proposed method can effectively preserve the details of the image while removing noise. Table 1 compares the performances of different image denoising methods. It can be seen that the proposed method has the smallest MSE and the largest SNR; i.e., it has the best denoising performance.

5 Conclusions

In this study, a new fractional-order integral denoising method has been proposed which uses the fractional gradient modulus to control the intensity of edge compensation. The fractional-order integral formula can be obtained by extending the integral order of the Cauchy integral formula from a positive integer to a positive real number. The slope approximation method has been used to realize the numerical calculation of the fractional Cauchy integral formula.

In the denoising process, the proposed method sets a higher order of small integral to construct the denoising mask in the increasing stage of SNR. At the beginning of the decrease of SNR, a lower order of the micro-integral has been set to construct the denoising mask, and an compensation mechanism has been used to partially restore the edge and texture information of the image. Simulation results showed that the proposed method has better denoising performance than the popular denoising methods based on the fractional-order integral theory. However, the noise reduction attained by fractional-order integral denoising methods should be compared with those of other denoising methods to find and establish the advantage and position of fractional-order theory in image processing. In future research, we need to focus on studying how to set the integral order, and try to select an appropriate value according to the local and non-local features of the image. In this way, we will be able to solve the problem of retaining edge and texture information in the process of image denoising.

Table 1 Performance comparison of Lena image processed by different image denoising models

Method	MSE	SNR (dB)	AG	EPI
Mean denoising	0.0049	14.6732	10.5327	2.3962
Gaussian	0.0042	15.6993	11.2498	2.8953
Wiener	0.0041	16.5922	11.3890	3.0242
G-L	0.0039	17.1527	12.0012	3.2189
PDE	0.0038	17.2315	11.8965	3.1682
NLM	0.0036	17.9212	13.6793	3.7639
Proposed method	0.0034	18.2165	13.5985	3.7038

Contributors

Li XU designed the research and drafted the manuscript. Guo HUANG and Qing-li CHEN processed the data. Guo HUANG, Hong-yin QIN, Tao MEN, and Yi-fei PU helped organize the manuscript. Li XU and Guo HUANG revised and finalized the paper.

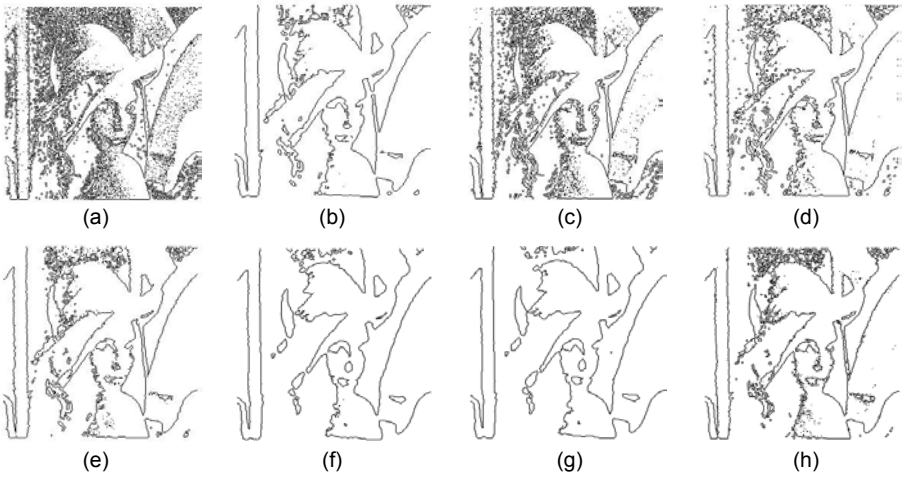

Fig. 4 Noise image (a) and horizontal line images obtained by the mean denoising method (b), Gaussian method (c), Wiener method (d), G-L method (e), PDE method (f), NLM method (g), and the proposed method (h)

Compliance with ethics guidelines

Li XU, Guo HUANG, Qing-li CHEN, Hong-yin QIN, Tao MEN, and Yi-fei PU declare that they have no conflict of interest.

References

Amoako-Yirenkyi P, Appati JK, Dontwi IK, 2016. A new construction of a fractional derivative mask for image edge analysis based on Riemann-Liouville fractional derivative. *Adv Differ Equat*, 2016:238. https://doi.org/10.1186/s13662-016-0946-8

Bai YR, Baleanu D, Wu GC, 2018. A novel shuffling technique based on fractional chaotic maps. *Optik*, 168:553-562. https://doi.org/10.1016/j.ijleo.2018.04.054

Bhrawy AH, Zaky MA, 2017. An improved collocation method for multi-dimensional space-time variable-order fractional Schrödinger equations. *Appl Numer Math*, 111: 197-218. https://doi.org/10.1016/j.apnum.2016.09.009

Chen DL, Sun SS, Zhang CR, 2013. Fractional-order TV-L^2 model for image denoising. *Cent Eur J Phys*, 11(10): 1414-1422. https://doi.org/10.2478/s11534-013-0241-1

Chen E, Min LQ, Chen GR, 2017. Discrete chaotic systems with one-line equilibria and their application to image encryption. *Int J Bifurc Chaos*, 27(3):1750046. https://doi.org/10.1142/S0218127417500468

Ding HF, Li CP, Yi Q, 2017. A new second-order midpoint approximation formula for Riemann-Liouville derivative: algorithm and its application. *IMA J Appl Math*, 82(5): 909-944. https://doi.org/10.1093/imamat/hxx019

He N, Wang JB, Zhang LL, et al., 2014. An improved fractional-order differentiation model for image denoising. *Signal Process*, 112:180-188. https://doi.org/10.1016/j.sigpro.2014.08.025

Huang G, Pu YF, Chen QL, et al., 2011. Research on image denoising based on fractional order integral. *Syst Eng Electron*, 33(4):925-932 (in Chinese). https://doi.org/10.3969/j.issn.1001-506X.2011.04.42

Jain S, Bajaj V, Kumar A, 2018. Riemann Liouvelle fractional integral based empirical mode decomposition for ECG denoising. *IEEE J Biomed Health Inform*, 22(4):1133-1139. https://doi.org/10.1109/JBHI.2017.2753321

Jalab HA, Ibrahim RW, 2015. Fractional Alexander polynomials for image denoising. *Signal Process*, 107:340-354. https://doi.org/10.1016/j.sigpro.2014.06.004

Jalab HA, Ibrahim RW, Ahmed A, 2017. Image denoising algorithm based on the convolution of fractional Tsallis entropy with the Riesz fractional derivative. *Neur Comput Appl*, 28(S1):217-223. https://doi.org/10.1007/s00521-016-2331-7

Jiang W, Wang ZX, 2012. Image denoising new method based on fractional partial differential equation. *Adv Mater Res*, 532-533:797-802. https://doi.org/10.4028/www.scientific.net/AMR.532-533.797

Li B, Xie W, 2016. Image enhancement and denoising algorithms based on adaptive fractional differential and integral. *Syst Eng Electron*, 38(1):185-192 (in Chinese). https://doi.org/10.3969/j.issn.1001-506X.2016.01.29

Liu ST, Yu L, Zhu BH, 2001. Optical image encryption by cascaded fractional Fourier transforms with random phase filtering. *Opt Commun*, 187(1-3):57-63. https://doi.org/10.1016/s0030-4018(00)01093-2

Liu Y, Pu YF, Zhou JL, 2011. A digital image denoising method based on fractional calculus. *J Sichuan Univ* (*Eng Sci Ed*), 43(3):90-95, 144 (in Chinese). https://doi.org/10.1016/j.cageo.2010.07.006

Liu ZJ, Liu ST, 2007. Double image encryption based on iterative fractional Fourier transform. *Opt Commun*, 275(2):324-329. https://doi.org/10.1016/j.optcom.2007.03.039

Nandal A, Gamboa-Rosales H, Dhaka A, et al., 2018. Image edge detection using fractional calculus with feature and contrast enhancement. *Circ Syst Signal Process*, 37(9):3946-3972. https://doi.org/10.1007/s00034-018-0751-6

Podlubny I, 1999. Fractional Differential Equations. Academic Press, New York, NY, USA, p.16-45.

Pu YF, Wang WX, Zhou JL, et al., 2008. Fractional differential approach to detecting textural features of digital image and its fractional differential filter implementation. *Sci China Ser F*, 51(9):1319-1339. https://doi.org/10.1007/s11432-008-0098-x

Pu YF, Siarry P, Zhou JL, et al., 2014. A fractional partial differential equation based multiscale denoising model for texture image. *Math Meth Appl Sci*, 37(12):1784-1806. https://doi.org/10.1002/mma.2935

Pu YF, Zhang N, Zhang Y, et al., 2016. A texture image denoising approach based on fractional developmental mathematics. *Patt Anal Appl*, 19(2):427-445. https://doi.org/10.1007/s10044-015-0477-z

Pu YF, Siarry P, Chatterjee A, et al., 2018. A fractional-order variational framework for retinex: fractional-order partial differential equation-based formulation for multi-scale nonlocal contrast enhancement with texture preserving. *IEEE Trans Image Process*, 27(3):1214-1229. https://doi.org/10.1109/TIP.2017.2779601

Shao L, Yan RM, Li XL, et al., 2014. From heuristic optimization to dictionary learning: a review and comprehensive comparison of image denoising algorithms. *IEEE Trans Cybern*, 44(7):1001-1013. https://doi.org/10.1109/TCYB.2013.2278548

Tian D, Xue DY, Wang DH, 2015. A fractional-order adaptive regularization primal–dual algorithm for image denoising. *Inform Sci*, 296:147-159. https://doi.org/10.1016/j.ins.2014.10.050

Wu GC, Zeng DQ, Baleanu D, 2019a. Fractional impulsive differential equations: exact solutions, integral equations and short memory case. *Frac Calc Appl Anal*, 22(1):180-192. https://doi.org/10.1515/fca-2019-0012

Wu GC, Deng ZG, Baleanu D, 2019b. New variable-order fractional chaotic systems for fast image encryption. *Chaos*, 29(8):083103. https://doi.org/10.1063/1.5096645

Wu XJ, Li Y, Kurths J, 2015. A new color image encryption

scheme using CML and a fractional-order chaotic system. *PLoS ONE*, 10(3):e0119660. https://doi.org/10.1371/journal.pone.0119660

Yu JM, Tan LJ, Zhou SB, et al., 2017. Image denoising algorithm based on entropy and adaptive fractional order calculus operator. *IEEE Access*, 5:12275-12285. https://doi.org/10.1109/access.2017.2718558

Zhang GM, Sun XX, Liu JX, 2016. Fractional total variation denoising model based on adaptive projection algorithm. *Patt Recogn Artif Intell*, 29(11):1009-1018 (in Chinese). https://doi.org/10.16451/j.cnki.issn1003-6059.201611006

Zhang J, Wei ZH, Xiao L, 2012. Adaptive fractional-order multi-scale method for image denoising. *J Math Imag Vis*, 43(1):39-49. https://doi.org/10.1007/s10851-011-0285-z